3.4

DEVELOPMENT OF NEW ICING PRODUCTS FOR SUPERCOOLED LARGE DROP CONDITIONS

Allyson Rugg*, Sarah Tessendorf, Darcy Jacobson, Dan Adriaansen, and Julie Haggerty
National Center for Atmospheric Research, Boulder, CO

1. INTRODUCTION

Supercooled large drops (SLD) pose a unique and, in some aircraft, enhanced threat to aviation safety compared to traditional small drop icing conditions due to their higher collision frequency, rougher texture, and ability to accumulate behind deicing boots (Cober and Isaac, 2012; Politovich 1989). In recent years, the Federal Aviation Administration (FAA) has imposed new icing regulations under 14 CFR Appendix O to Part 25 to address hazards associated with SLD icing conditions, augmenting existing regulations regarding small drop icing conditions in Appendix C. Appendix O SLD conditions, defined as drops of at least 100 μm in diameter, are further broken down by the maximum supercooled liquid drop diameter (DMax) into freezing drizzle (100μm<DMax<500μm; FZDZ) and freezing rain (DMax>500μm; FZRA). These new regulations and associated environmental categories have necessitated research on how to provide operational drop size guidance to the aviation community.

The availability of more sophisticated Numerical Weather Prediction (NWP) models along with improved observational networks facilitate development of icing weather tools with enhanced capability for classifying drop size. Specifically, the High Resolution Rapid Refresh model (HRRR), running operationally at the National Center for Environmental Prediction, features the Thompson-Eidhammer aerosol-aware bulk microphysics parameterization (Thompson and Eidhammer 2014), which provides forecasts of both mixing ratio and number concentration for the cloud and rain hydrometeor categories. Using these predicted quantities, the DMax is allowed to vary under different conditions in the model forecast. Deriving DMax from the model forecast can be used to advance operational icing tools, such as the Current Icing Product (CIP) and Forecast Icing Product (FIP), to address Appendix O.

This paper describes the approach used to distinguish small and large drop icing conditions and further categorize the SLD conditions based on drop size in support of Appendix O regulations. The HRRR-based drop size forecasts are compared to *in situ* aircraft measurements from research flights in Idaho to evaluate the capability of the model to accurately distinguish small drop icing, freezing drizzle, and freezing rain.

* *Corresponding author address:* Allyson Rugg, 3450 Mitchell Ln, Boulder CO 80301; email: arugg@ucar.edu

2. DATA AND METHODS

2.1 HIGH RESOLUTION RAPID REFRESH MODEL (HRRR)

In the operational HRRR, which runs the Thompson-Eidhammer aerosol-aware bulk microphysics scheme, the rain drop hydrometeor category encompasses both drizzle and rain sized drops, as defined by Appendix O, while the cloud drop hydrometeor category includes only small drop (Appendix C) supercooled liquid (Thompson and Eidhammer, 2014). The size distribution, N(D), of the rain/drizzle drops is parameterized with the ratio of total number concentration, N_t, and the mass mixing ratio, q, using an exponential probability distribution:

$$N(D) = \lambda e^{-D\lambda}$$

$$\lambda = \left(\frac{\pi \rho N_t}{q}\right)^{1/3}$$

Where D is the drop diameter and ρ is the density of liquid water. Because the exponential probability distribution is infinite, it is difficult to determine what the maximum drop size is--any drop size is possible, though the probability of

observing a drop becomes infinitesimal with its increasing diameter.

Research presented by Tessendorf et al. (2017) suggested the 99th percentile of the distribution as an appropriate estimate of maximum diameter. This way, one percent of the modeled raindrops are at least as large as DMax. Figure 1 illustrates this 99th percentile method with an example size distribution from the HRRR. The blue curve shows the modeled size distribution, while the dashed lines indicate the 50th, 70th, 95th, and 99th percentiles of the number concentration. The key size thresholds for regulations (100μm and 500μm) are also marked as solid gray lines. In this example, the 99th percentile, and thus the DMax, is just over 500μm, which would classify this case as freezing rain.

The Inflight Icing (IFI) team at the National Center for Atmospheric Research (NCAR) has used this 99th percentile method product to create an experimental DMax and Appendix C/O classification product in real time over the Contiguous United States (CONUS). Figure 2 shows an example of the composite (column max) DMax product over the Carolinas during a winter storm on 10 December 2018 that produced ample snowfall in Virginia. The warm colors indicate areas of freezing rain, while cooler colors indicate freezing drizzle. This product has shown skill in distinguishing freezing drizzle from freezing rain in isolated cases (Tessendorf et al., 2017) but this study will provide a more comprehensive evaluation of its strengths and weakness by comparing it to *in situ* observations.

To limit the amount of data processing required, but not rely on a single forecast lead time, the 3, 6, and 12-hour forecasts are considered for this study. The 3-hour forecast is considered because it is used in the Current Icing Product (CIP), which runs operationally in real time providing icing

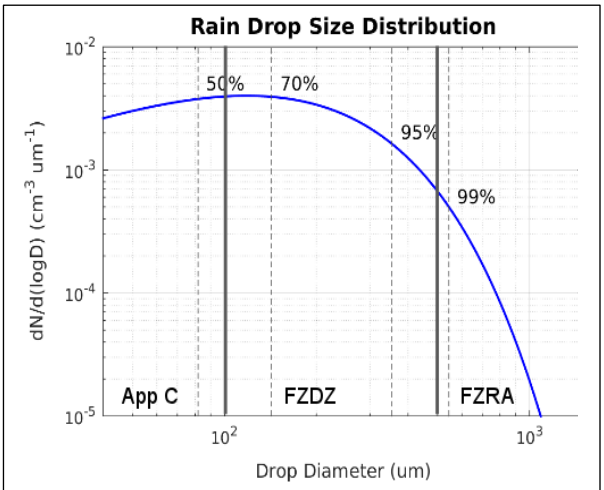

Figure 1: An example raindrop size distribution from the HRRR (blue) with various percentiles of the distribution marked as dashed lines. The critical 100μm and 500μm DMax thresholds are also indicated as solid gray lines. In this case, the 99th percentile, or DMax, is just above 500μm, classifying the distribution as freezing rain.

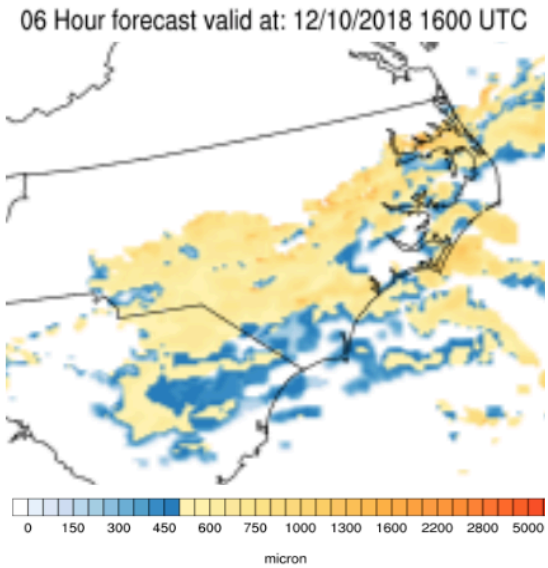

Figure 2: Example of the experimental DMax product from the 6-hour HRRR forecast valid at 1600 UTC on 10 December 2018 over the Carolinas. The maximum diameter (shading) is represented the 99th percentile of the model raindrop hydrometeor category, and the composite (column maximum) is shown in this image. Areas falling into the Appendix O freezing rain category are shown in warm/orange colors, while those categorized as freezing drizzle are shown in cool/blue colors.

probability and severity. The 12-hour lead time is chosen because case studies have previously shown that longer lead times occasionally resolve SLD conditions more accurately than shorter lead times. The 6-hour lead time is also used to provide a mid-range forecast. Future work may more formally evaluate the HRRR's ability to forecast SLD as a function of lead time, but this study will consider these three lead times simultaneously.

2.2 IN SITU OBSERVATIONS

In situ observations of hydrometeor sizes are not routinely collected and are isolated to field campaigns, usually with cloud imaging probes on board research aircraft. Observations of supercooled large drops are even more infrequent since these conditions are only present in a subset of the clouds sampled. Fortunately, the recent Seeded and Natural Orographic Wintertime clouds: the Idaho Experiment (SNOWIE) which took place in January to March of 2017 in the Payette River basin north of Boise, Idaho, included several cases with SLD and in situ observations of drop size (Tessendorf et al., 2019).

For this study, particle sizes from the onboard 2D-S imaging probe were compared to the HRRR DMax product. Because part of the SNOWIE project was to evaluate the impact of cloud seeding by silver iodide, only flight legs occurring in natural clouds (i.e. before seeding was conducted) were used in study. For these segments, from a total of eight different flights, the 2D-S images were processed to remove shattered pieces, particles under 50μm which are too small to reliably classify as liquid or ice, and other artifacts. The largest particle the 2D-S is capable of observing is 1260μm in diameter, but the vast majority of liquid particles were well below this threshold. Since whole particles can appear as hollow rings when out of focus, these holes were filled, and then the diameters, areas, and perimeters of each particle computed. A shape parameter was then defined as the product of the diameter and perimeter divided by the area. For a perfect circle this shape parameter is four, but anything under 5.65 was considered circular and therefore liquid for this study. This threshold was determined by visually examining particles from several all-liquid and all-ice cases and the overall distribution of shape parameters.

Having separated liquid particles from snow and ice, the observations were grouped into 30-second windows to roughly match the 3-km grid spacing of the HRRR at an airspeed of 100m/s. If a 30-second window (hereafter just "observation") included fewer than 100 liquid particles, it was omitted from analysis, otherwise the 99th percentile of the observed diameters was used as the observed DMax. Various other methods were evaluated for computing the DMax from the observations, including the diameter of the largest particle, and diameter of the 10th largest particle. The latter of these methods is most similar to methods used in Cober and Isaac (2012) which was used in the development of Appendix O regulations. These three methods yielded similar values and the 99th percentile was chosen to match the method applied to the HRRR.

The distribution of observed DMax is shown in Figure 3. In total there were 73 Appendix C small drop icing observations, 209 freezing drizzle observations, and 2 freezing rain observations. The absence of a warm nose in both the model

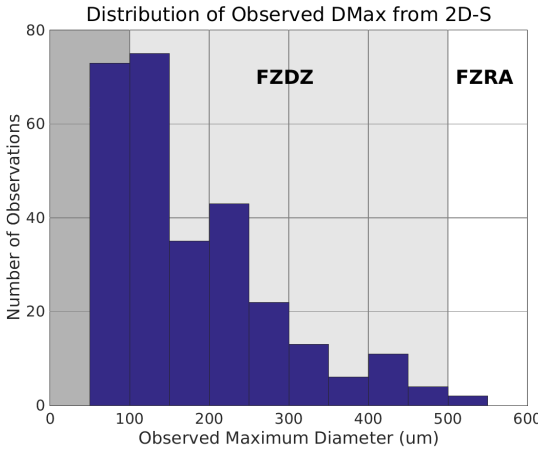

Figure 3: The distribution of observed DMax from the 2D-S after removing shattered pieces, particles under 50μm, and observations with fewer than 100 total liquid particles. There was a total of 73 Appendix C (small drop) observations, 209 freezing drizzle, and 2 freezing rain.

and nearby observed atmospheric profiles suggests the SLD was “non-classical” and driven by collision and coalescence (not shown).

3. RESULTS

Initial analysis revealed high spatial variability regarding the presence of explicit rain water in the HRRR. For example, Figure 4 shows a composite image of where the HRRR had supercooled rain/drizzle (shading, lighter blues indicate more rain) for the 12-hour forecast valid at 0400 UTC on 9 January 2017 with the flight path overlaid as a dark red line. Previous studies have also shown that point-by-point matching of high-resolution model output to point observations is not a reliable evaluation method since models are often slightly off in the location of features (Rossa et al, 2008). As such, small neighborhoods of model grid cells centered around the observations are often used for comparison. While several neighborhood sizes were considered, the remainder of this study will focus on results using a neighborhood of 5 by 5 model cells (+/- 2 from the nearest point giving 15 by 15 km box) in the horizontal and 3 vertical levels (+/- 1 from flight level). This has the added benefit of providing more data for analysis since the HRRR DMax cannot be computed unless there is explicit supercooled rain water. By using every point in the 5 by 5 by 3 neighborhood, along with 3 lead times, each observation is matched to 225 different model points. The probability of detection (POD) for SLD, defined as the percent of time at least one of those 225 model points forecasted SLD when it was observed, was 18.2%.

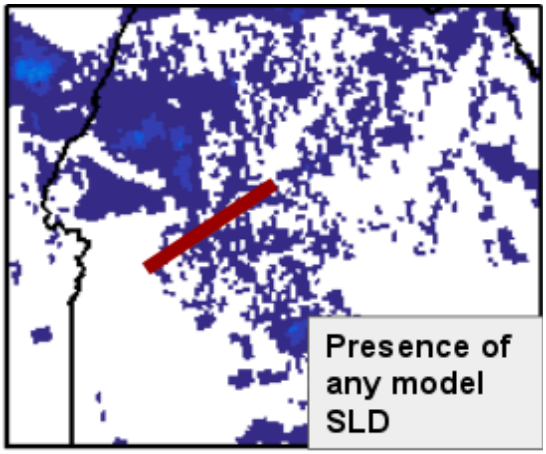

Figure 4: Composite (column max) supercooled rain mixing ratio from the HRRR (shading, lighter shades of blue indicate higher mixing ratio). Image shown is from a 12-hour forecast valid at 0400 UTC on 9 January 2017. The dark red line indicates the flight path. White space is where no SLD was predicted, though almost the entire flight observed SLD in this case.

Figure 5 summarizes the HRRR DMax performance where the colors indicate the number of observation-HRRR pairs with a given range of Dmax values. Essentially, the warmer colors indicate more dense points on a scatter plot. Observations are plotted once for every matching HRRR point with SLD in the 5 by 5 by 3 neighborhood, so if all HRRR points had SLD, the same observation would be plotted 225 times. One encouraging result is that the model DMax (y-axis) spans the whole range from Appendix C to FZRA sizes. This demonstrates that, despite having a fixed size distribution functional (exponential) form with an infinite maximum size, the model microphysics parameterization is capable of producing the full range of maximum diameters critical to Appendix O using the 99th percentile approach to deriving DMax. However, the accuracy of the predicted DMax when supercooled rain is predicted by the HRRR forecast model needs improvement. Though the range of HRRR DMax values is large, the cluster of yellow, green, and light blue boxes on the left hand side of the plot indicates a narrow distribution of HRRR DMax values centered around 300μm. Compared to observations largely below 300μm, the HRRR DMax has a high root mean squared error (RMSE) of 235 microns. Because the model generally overestimates the DMax (most points are above the black one-to-one line), there is a low rate of under-categorizing FZDZ as Appendix C (2.5%), but a high rate of over-categorizing Appendix C as FZDZ (99%). These statistics, however, still rely on the model producing some amount of supercooled rain water, which was not usually the case (POD of 18.2%).

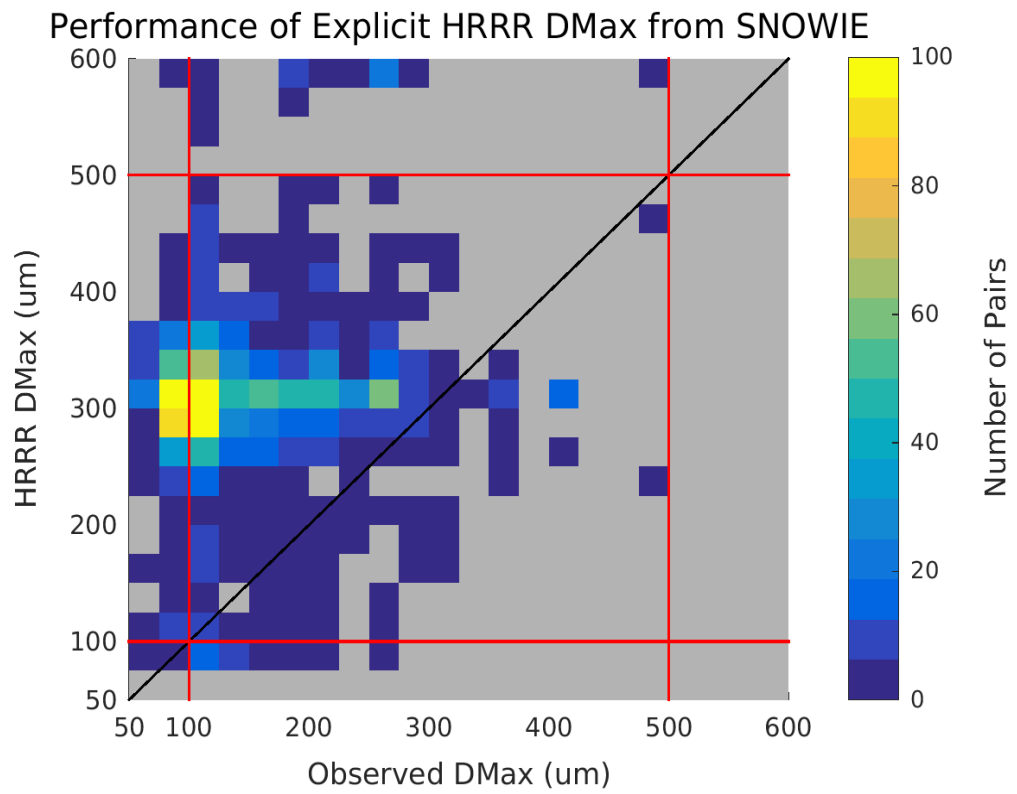

Figure 5: DMax values from observations and the HRRR were binned every 25μm between 50 and 600μm. The colors indicate the number of pairs that fell into a bin (gray indicates zero). Red lines highlight the critical 100μm and 500μm size thresholds for FZDZ and FZRA. Black line represents a perfect match between observations and model. Observations are counted up to 225 times, once for every matching HRRR grid point that had SLD (5 by 5 grid points in the horizontal, 3 grid points in the vertical, 3 lead times).

There are several possibilities for why the model missed so much SLD and had a high error in the DMax that did exist. These include errors in the driving dynamics, unrepresentative background aerosol forcings, and overproduction of snow/ice which would deplete supercooled liquid and thus limit SLD. In addition, the model prescribes an exponential size distribution for the rain category which may affect the accuracy of the resulting DMax.

3.1 EVALUATION OF PRESCRIBED EXPONENTIAL RAIN DROP SIZE DISTRIBUTION

To quantify the impact of the prescribed exponential form of the drop size distribution (DSD), such function was fit to the observed distribution using the maximum likelihood method. The DMax (99th percentile) of the resulting exponential distribution was then extracted and compared to the observed DMax. This is illustrated in Figure 6, where the black curve represents the exponential DSD fitted to the observed drops sizes, which were then binned and plotted as blue bars. The inset shows the observed DMax (red bar) and the DMax from the fitted curve (red dot) for this example. The functional form of the distribution is also shown in the top left where N(D) is the probability distribution of drop sizes, D is the drop diameter, and λ is the parameter optimized to produce the fitted black curve.

Figure 7 shows how these approximated DMax values compare to the observed ones. It is important to remember that no model output is

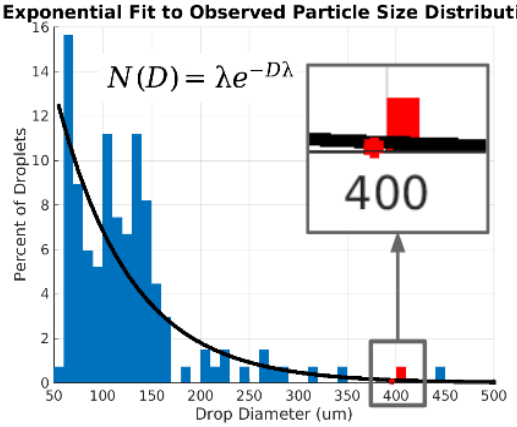

Figure 6: Example of an observed drop size distribution (blue bars) and the maximum likelihood exponential fit to that distribution (black curve). Equation in the top left shows the general form of the exponential fit where N(D) is the probability density of a particle having diameter D, and λ is the parameter adjusted to fit the function to observations. The insert on the right shows the observed (red bar) and approximated (red circle) DMax.

shown in this figure. The x-axis is the observed DMax, while the y-axis is the DMax from an exponential function fitted to those same observations. The figure does not show model performance, but rather how well a DMax can be approximated using an exponential drop size distribution. This can be conceptualized as the minimum error the model could achieve with this prescribed form of the DSD. With a root mean squared error (RMSE) of 69μm, the constraints of this functional form could account for up to 30% of the error in HRRR DMax (Figure 5). It is worth noting that the fitted exponential functions tend to overestimate DMax when the observed values are small, as seen by most of the blue dots being above the gray one-to-one line when the observed values are less than 150μm. While the errors are still much smaller than those seen in Figure 5, this could contribute to the overestimation of DMax when SLD is present in the model. At larger observed DMax values there is no obvious bias, but the errors become much larger (blue dots further from the gray line). This may be due to observed bimodal distributions from collision-coalescence processes at larger sizes which are not well approximated by exponential distributions. While Figure 7 shows all observations, results were very similar when only points where the HRRR contained SLD were considered (not shown). In general, it appears the prescribed exponential form of the DSD in the HRRR is an appropriate approximation for observed distributions and the errors in modeled DMax largely originate elsewhere.

3.2 POSSIBLE AEROSOL IMPACTS

It is well known that aerosols impact the number and sizes of cloud drops; as aerosol concentrations increase, droplets generally become smaller but more numerous as there are more particles on which water can condense. As such, it was hypothesized that the collision and coalescence of cloud drops into SLD sizes may have been inhibited in the model by higher than observed aerosol concentrations. This could explain the low probability of detection of FZDZ or FZRA sized drops.

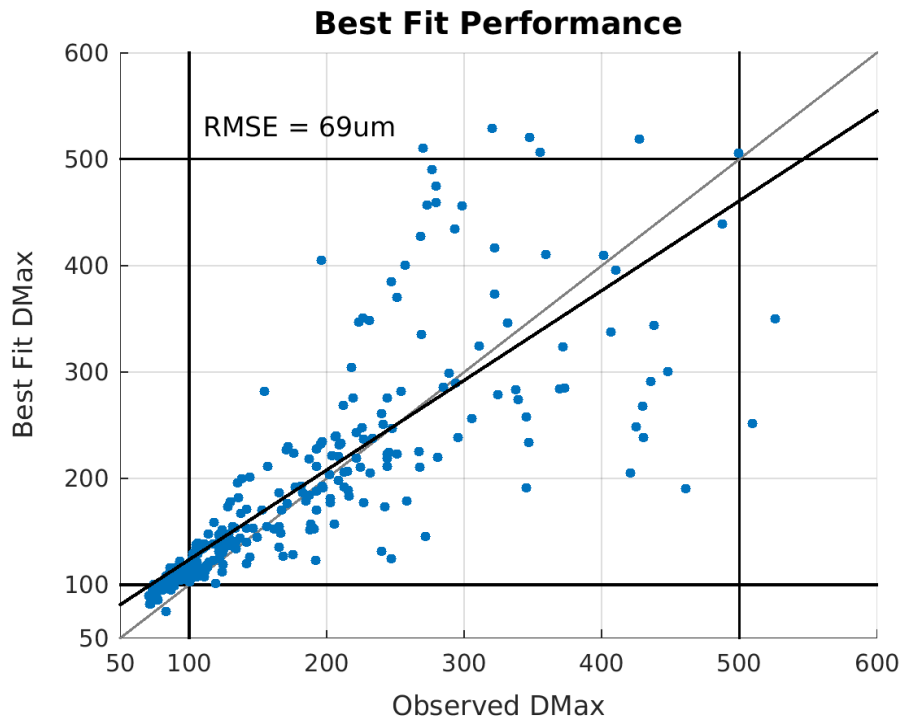

Figure 7: Exponential functions were fit to observed size distributions (see Figure 6 and text) and the 99th percentiles of these functions compared back to the observed DMax values (blue dots). The diagonal black line is the least squares line of best fit between the observed and approximated DMax values. The gray line shows the one-to-one line which would represent a perfect exponential fit to the observations. The root mean squared error (RMSE) was 69um.

The SNOWIE campaign lacks *in situ* aerosol measurements, but cloud droplet number concentration from the cloud droplet probe (CDP) can be compared to the HRRR cloud number concentrations as a proxy for aerosol content since smaller, more numerous drops are generally indicative of higher aerosol concentrations. Figure 8 shows the comparison of these cloud drop number concentrations from the observations (blue), and the HRRR (red). Compared to observations, the model had fewer instances of very low drop concentration (0-40 drops per cubic centimeter), and higher rates of concentrations greater than 60 drops per cubic centimeter. This supports the hypothesis that part of the underproduction of SLD in the model could be from higher than observed background model aerosol contents.

4. SUMMARY AND CONCLUSIONS

Using *in situ* drop size measurements and cloud drop number concentrations in Appendix C and Appendix O freezing drizzle icing environments from eight SNOWIE flights, the ability of the High Resolution Rapid Refresh model (HRRR) to accurately forecast the maximum supercooled liquid drop diameter (DMax) was evaluated. Observed DMax was computed as the 99th percentile of the drop diameters observed in a 30-second window from a 2D-S probe. These observations were compared to the 99th percentile of the exponential distribution of modeled rain drop sizes from the Thompson-Eidhammer aerosol-aware microphysics scheme in the HRRR. Overall the model had a 18.2% probability of detecting observed SLD conditions.

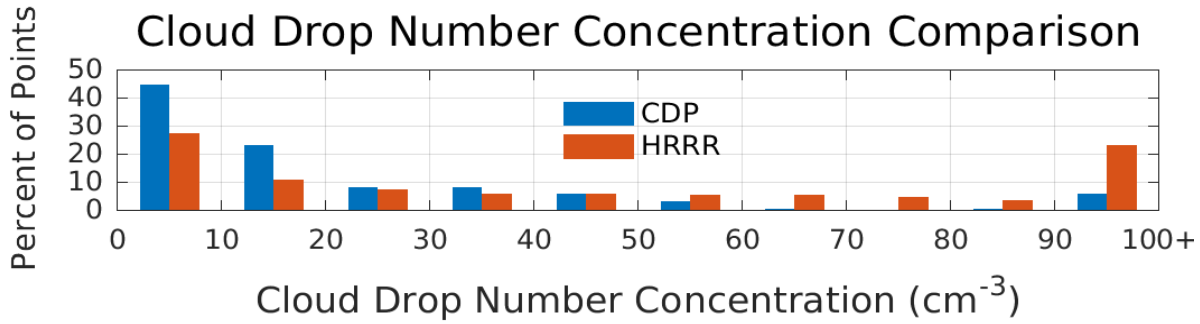

Figure 8: Cloud drop number concentrations (number of drops per cubic centimeter) from the in situ cloud droplet probe (blue; CDP) and from the HRRR (red). The observed concentrations were generally lower than modeled.

The distribution of model DMax values demonstrates the model is capable of producing the full range of sizes applicable to icing regulations--from Appendix C small drop icing (<100μm) to Appendix O freezing drizzle (>100μm and <500μm) and freezing rain (>500μm). The ability for the model to produce a DMax that falls into the freezing drizzle size range is especially notable. This signifies that the two-moment microphysics scheme for the rain hydrometeor category, even with an infinite and fixed functional form for the size distribution, is capable of becoming narrow enough such that drizzle situations are simulated. Thus, the HRRR model microphysics are capable of distinguishing freezing drizzle from freezing rain for the purposes of categorizing Appendix O conditions. However, this analysis revealed that the model DMax, when SLD was predicted, was generally larger than observations, and the model's ability to produce SLD in general needs to be improved.

Two factors that could contribute to these errors in the model were investigated: the prescribed form of the size distribution and the model aerosol forcing. Because the model prescribes an exponential drop size distribution, such function was fit to observations to assess the appropriateness of this functional form. The DMax produced by these fitted exponential distributions produced a root mean squared error 30% as large as that from the modeled DMax, showing that most of the model's error lies elsewhere. Cloud drop number concentrations from an *in situ* cloud droplet probe and from the model were compared to see if the model aerosol content could have been responsible for less SLD in the model. Indeed, the distribution of modeled cloud drop concentrations was weighted towards higher concentrations than observed, which could contribute to the model's underproduction of SLD conditions. Nonetheless, there are still a variety of other factors that could cause the model's underproduction of SLD and require further investigation.

5. FUTURE WORK

There remain many unexplored reasons why the HRRR model had a low probability of detecting SLD (18.2%), and why the cases that did produce SLD had a bias towards larger than observed DMax values. Future research will explore additional factors, such as over production of snow and ice which would deplete supercooled liquid and thus SLD and has been seen in previous case studies. An evaluation of the driving atmospheric dynamics is also needed because the model microphysics is heavily dependent on the performance of the larger scale synoptic and mesoscale conditions. As more is discovered about the model strengths and weaknesses, algorithms will be developed to compensate and provide products tuned to the needs of the aviation community. Such algorithms will likely incorporate fuzzy logic similar to the Forecast Icing Product which runs operationally on the WRF-RAP model.

In addition to further exploration of model limitations, additional *in situ* data are required to expand the types of conditions observed. The SNOWIE campaign has provided valuable data in

orographically-driven freezing drizzle, but the data are limited geographically to the Boise, Idaho area and include very few cases with freezing rain sized drops. These deficiencies in the available data will be addressed using observations from the Buffalo Area Icing and Radar Study II (BAIRS-II) which took place near Buffalo, New York from January to March of 2017, and the In-Cloud Icing and Large-drop Experiment (ICICLE) planned for January to March 2019 out of Rockford, Illinois.

ACKNOWLEDGEMENTS

This research is in response to requirements and funding by the Federal Aviation Administration (FAA). The views expressed are those of the authors and do not necessarily represent the official policy or position of the FAA.

REFERENCES

Cober, S.G. and G.A. Isaac, 2012: Characterization of Aircraft Icing Environments with Supercooled Large Drops for Application to Commercial Aircraft Certification.*J. Appl. Meteor. Climatol.,* **51**, 265–284, https://doi.org/10.1175/JAMC-D-11-022.1

Politovich, M.K., 1989: Aircraft Icing Caused by Large Supercooled Droplets. *J. Appl. Meteor.,* **28**, 856–868, https://doi.org/10.1175/1520-0450(1989)028<0856:AICBLS>2.0.CO;2

Rossa A., Nurmi P., Ebert E., 2008: Overview of methods for the verification of quantitative precipitation forecasts. In: Michaelides S. (eds) Precipitation: Advances in Measurement, Estimation and Prediction. Springer, Berlin, Heidelberg

Tessendorf, S. A, D. R. Adriaansen, A. Rugg, D. Serke, C. Williams, J. Haggerty, G. Cunning, G. McCabe, P. Prestopnik, G. Thompson, and J. Kenyon, 2017: Developing Improved Products to Forecast and Diagnose Aircraft Icing Conditions Based upon Drop Size. *9th AIAA Atmospheric and Space Environments Conference.* Denver, Colorado.

Tessendorf, S.A., J.R. French, K. Friedrich, B. Geerts, R.M. Rauber, R.M. Rasmussen, L. Xue, K. Ikeda, D.R. Blestrud, M.L. Kunkel, S. Parkinson, J.R. Snider, J. Aikins, S. Faber, A. Majewski, C. Grasmick, P.T. Bergmaier, A. Janiszeski, A. Springer, C. Weeks, D.J. Serke, and R. Bruintjes, 2019: Transformational approach to winter orographic weather modification research: The SNOWIE Project. *Bull. Amer. Meteor. Soc.*, **0**, https://doi.org/10.1175/BAMS-D-17-0152.1

Thompson, G. and T. Eidhammer, 2014: A Study of Aerosol Impacts on Clouds and Precipitation Development in a Large Winter Cyclone. *J. Atmos. Sci.,* **71**, 3636–3658,https://doi.org/10.1175/JAS-D-13-0305.1